Regeneration, Reconstruction & Restoration

Original Article

Open Access

Assessing the Variations of the Depth and Angle of the Submandibular Gland Fossa and the Mandibular Canal Using Cone Beam Computed Tomography (CBCT)

Alireza Khodabakhshian[a], Melika Mollaei[a], Mona Alimohammadi[b], Fatemeh Ghobadi[b], Abolfazl Hosseinnataj[c], Atefeh Gholampour[b*]

[a]Dental Research Center, Student Research Committee, Faculty of Dentistry, Mazandaran University of Medical Sciences, Sari, Iran; [b]Department of Oral and Maxillofacial Radiology, Dental Research Center, Faculty of Dentistry, Mazandaran University of Medical Sciences, Sari, Iran; [c]Department of Biostatistics, Faculty of Health, Mazandaran University of Medical Sciences, Sari, Iran.

Corresponding authors:** Atefeh Gholampour, Department of Oral and Maxillofacial Radiology, Dental Research Center, School of Dentistry, Mazandaran University of Medical Sciences, Sari, Iran. ***E-mail: atefehgholampour70@yahoo.com ***Tel:*** +98 910 102 2013

Submitted: 2 January, 2024**; Accepted:** 12 March, 2024**; Published Online:** 5 May, 2024**; DOI:** *10.22037/rrr.v9.44263*

Background and objectives: The most important anatomical areas to take into account during implant insertion are the submandibular gland cavity, the posterior part of the mandible, and the inferior alveolar nerve. Therefore, this study aims to assess the location of the submandibular gland fossa and its variations using CBCT.

Materials and methods: In this cross-sectional investigation, CBCT images of the mandible of patients who visited a private radiology center in Babol (Mazandaran, Iran) between 2019 and 2021 were included. The submandibular salivary gland fossa was evaluated based on age, sex, side of the mandible, fossa depth and angle, as well as connection with the mental foramen and mandibular canal. Data were analyzed using SPSS V.24.

Results: The study population comprised 59 men (47.2%) and 66 (52.8%) women, ranging from 16 to 70 years old. The mean depth of the fossa on the right side (1.79 ± 0.48 mm) was statistically greater than the left side (1.66 ± 0.46 mm). Regarding the angle of the fossa and the distance to the mental foramen, there was no discernible difference between the left and right sides. Men had considerably deeper average fossa depths on both sides ($P<0.05$). Moreover, the fossa depth on the right side was significantly lower in patients less than 36 years old ($P=0.005$).

Conclusion: According to the current findings, the average depth of the fossa is greater on the right side than on the left side. The deepest part of the fossa is located next to the mandibular canal. Therefore, it is crucial to have a thorough understanding of the characteristics of the submandibular gland fossa to avoid perforating the lingual alveolar plate during implant insertion.

Keywords: Cone Beam Computed Tomography, CBCT, Dental implant, Submandibular gland fossa.

1. Introduction

Implant placement is one of the most critical dental surgeries for replacing missing teeth. Anatomical landmarks are crucial variables that should be considered while placing implants [1]. Bone perforation is one of the consequences of dental implant failure, which is caused by infection and inflammation [2].
The posterior region of the mandible, the submandibular gland cavity, and the inferior alveolar nerve are the most essential anatomical regions, since the submental and sublingual arteries pass through them. During surgery, damage to the inferior alveolar canal leads to paresthesia or numbness surrounding the mouth and chin [3, 4].
The submandibular salivary glands are a pair of major salivary glands located under the oral cavity floor. They are positioned in the anterior part of the submandibular triangle. The submandibular gland fossa is a concavity in the internal part of the mandible trunk under the mylohyoid line and the mandibular canal, which is often adjacent to the inferior border of the mandible. This concavity is under the internal oblique line on both sides and appears as a radiolucent area with a scattered trabecular pattern in radiographic images [5]. Lingual plate

perforation damaging the submandibular gland fossa can cause severe bleeding and a subsequent hematoma, which can be fatal owing to airway obstruction [6].
In order to assess different anatomical areas, various evaluations, such as palpation of the ridges and diagnostic casts are performed before implant placement. However, the posterior mandibular area cannot be evaluated with these modalities. Therefore, Cone beam computed tomography (CBCT) is a suitable diagnostic technology that can identify the status of the concavities and result in an acceptable fixture [7, 8].
CBCT provides high-resolution and accurate 3D images for implant planning. However, the evaluation of the submandibular gland fossa has resulted in controversies among different investigations [9, 10]. Sushmitha et al. suggested that the mean fossa depth was significantly higher in women [11], while other studies discovered that men had significantly higher fossa depth [4, 12]. Considering the existing controversies, this investigation evaluates the angle and depth of the submandibular gland fossa as well as the mandibular canal using CBCT.

2. Materials and methods

This cross-sectional study collected the CBCT radiographs of patients referred to a private oral and maxillofacial radiology center in Babol, Mazandaran, Iran, between 2019-2021. The Mazandaran University of Medical Sciences ethics committee approved the study protocol (code: IR.MAZUMS.REC.1401.167). The sample size was calculated based on Haghanifar et al.'s study [4], as well as the confidence level of 95% and the test power of 90% in the formula as demonstrated:

$$n = \frac{\left(z_{1-\frac{\alpha}{2}} + z_{1-\beta}\right)^2 * \sigma^2}{(d)^2}$$

A total number of 125 CBCT images (250 sides of the mandible) of patients with complete or partial edentulism ridges in the posterior area of the mandible were included. The patients had an age range of 16 to 70 and were already exposed to radiation for diagnostic proposes. Individuals with developmental and congenital disorders, abnormal morphology caused by trauma, and pathologies affecting the target region were excluded [13].
All images were prepared and reconstructed using NewTom Giano (Verona, Italy) and NNT software (Verona, Italy). Exposure conditions included a field of view (FOV) of 11×8cm, 90 kvp, 10 mA, and a Voxel size of 100 µm. The measurements were recorded three times by a senior dental student and the mean was calculated. All measurements were performed under the supervision of a radiologist.
The morphology of the submandibular fossa was examined using panoramic and cross-sectional sections (slice thickness=1 mm). The location of the infra-alveolar canal was detected in the panoramic images. The fossa of the infra-alveolar gland was also detected in the cross-sectional radiographs (thickness and interval of 1 mm), and the deepest area of the fossa was located [13].
The fossa depth determination: Line A was drawn connecting the highest and lowest points of the fossa. Line B was drawn from the deepest area of the fossa of the submandibular gland perpendicular to line A (Figure 1). The depth of the fossa was determined according to the size of line B [4].
The association of the fossa with the infra-alveolar canal was assessed in three groups based on the location of this line compared to the infra-alveolar:

1. Superior relation: The deepest point of the fossa is located above the mandibular canal.
2. Parallel relation: The deepest point of the fossa is next to the mandibular canal.
3. Inferior relation: The deepest point of the fossa is below the mandibular canal [13].

The concavity angle determination: A tangent line was considered on the superior point of the concavity and perpendicular to the horizon (Line C), as well as another line on the superior wall of the concavity in contact with the superior point and the deepest point of the fossa (Line D). The angle between lines C and D was calculated (Figure 2) [4].
The starting point of the undercut determination: a tangent line on the superior wall of the channel and parallel to the horizon was drawn (line E). Line F was also drawn tangent to the ridge and parallel to line E (Figure 3). The distance between E and F lines was divided into 3 sections: 1/3 coronal, 1/3 middle, 1/3 apical. The undercut starting point was placed in one of these 3 sections (Figure 3) [4].
The distance from the fossa to the mental foramen: In the panoramic view, it was determined how far the deepest section of the fossa was from the distal wall of the mental foramen. (Figure 4) [13].
Statistical analysis was conducted using SPSS 24 software. Mean, standard deviation, percentage, and chi-score statistical tests were used for data analysis. A p-value less than 0.05 was considered statistically significant.

3. Results

125 CBCT images (59 male and 66 female) were studied. The patients had a mean age of 40.75 ± 9.71 years old (ranging from 23 to 65). More than half of the patients (52%) were between 36 and 50 years old. As observed in Table 1, findings revealed that the mean depth of the fossa on the right side of the mandible was remarkably greater than the left side (P=0.037). Between the right and left sides, there was no statistically significant disparity n terms of fossa angle and distance to the mental foramen (P=0.163 and P=0.488, respectively). The correlation coefficient

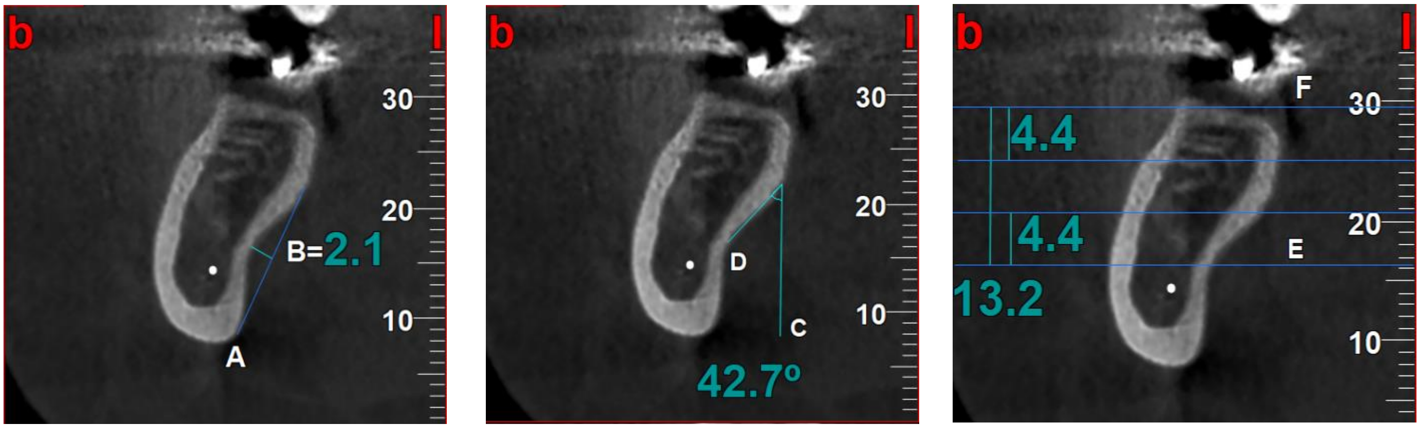

Figure 1. Cross-sectional CBCT view measuring the depth of the fossa (left), Cross-sectional CBCT view measuring the angle of the fossa (middle), Cross-sectional CBCT view measuring the starting point of the undercut (right).

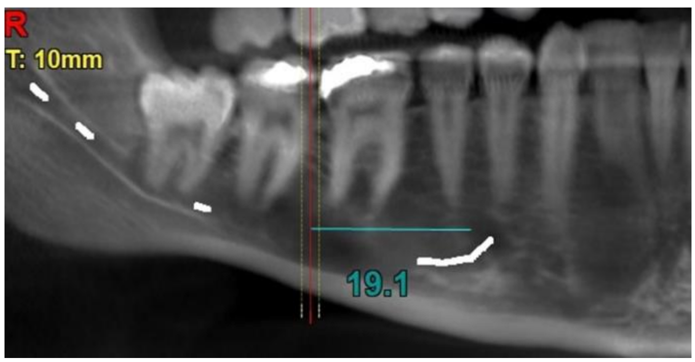

Figure 2. Measuring the distance from the fossa to the mental foramen.

between the fossa depth and fossa angle was positive and significant on both sides; therefore, with the increase in the fossa's depth, the angle of the fossa also increased ($P<0.001$).
The average depth of the fossa on both sides had a significant association with sex and was higher in men compared to women. Additionally, the average fossa angle and the separation between the mental foramen and the deepest point of the fossa had no significant relation with sex (Table 2).
Moreover, the average depth of the fossa in the right direction had a significant relationship with age and was lower in people under 36 years old ($P=0.005$). The average depth of the left fossa was borderline related ($P=0.050$). The mean fossa angle and the separation between the mental foramen and the deepest point of the fossa had no significant relationship with the age ($P>0.05$), as observed in Table 3.
According to Table 4, the deepest part of the fossa on the right and left sides was located next to the mandibular canal, and the patients were not significantly different in terms of sex. Furthermore, the beginning of concavity on the right and left sides was mostly in the middle 1/3, and no significant disparity was observed between men and women (Table 5).

4. Discussion

Dentists have a wide range of options for assessing the jaw's health prior to dental implant treatment. Many techniques, such as clinical palpation, osteometers, diagnostic casts, and conventional radiography, have been employed for this purpose. However, utilizing these technologies for pre-implant testing has limitations. For instance, the sub-mylohyoid and the floor of the mouth cannot be measured using osteometers and casts, respectively. Clinical palpation can help in diagnosis but may not be effective in complete identification. Therefore, preoperative imaging is essential for successful implant placement [8].
When evaluating the mandible before surgery to insert implants, CBCT imaging offers precise information on the mandibular architecture and the depth of the submandibular gland cavity.
The findings of this research suggest that the mean depth of the fossa on the right side of the mandible is remarkebly depeer than the left side. Moreover, a significant asssociation between the depth and the angle of the fossa was also found on both sides and

Table 1. Demographic features of the fossa depth, angle, and distance to mental foramen.

Variable	Side	Mean ± standard deviation	P-value
Fossa depth	Right	1.79 ± 0.48	0.037
	Left	1.66 ± 0.46	
Fossa angle	Right	41.24 ± 5.04	0.163
	Left	40.36 ± 4.83	
Distance to mental foramen	Right	16.70 ± 1.96	0.488
	Left	16.52 ± 2.25	

Table 2. Measurements of fossa depth, fossa angle, and the distance of the deepest part of the fossa to the mental foramen onn both sides based on the patients' sex.

Variable	Side	Sex	Mean ± standard deviation	P-value
Fossa depth	Right	Male	1.90 ± 0.45	0.009
		Female	1.68 ± 0.49	
	Left	Male	1.79 ± 0.45	0.002
		Female	1.55 ± 0.43	
Fossa angle	Right	Male	41.54 ± 4.71	0.533
		Female	40.97 ± 5.34	
	Left	Male	4.63 ± 4.20	0.572
		Female	40.13 ± 5.35	
Distance to mental foramen	Right	Male	16.63 ± 1.89	0.702
		Female	16.77 ± 2.04	
	Left	Male	16.48 ± 2.21	0.870
		Female	16.55 ± 2.29	

Table 3. Measurements of fossa depth, fossa angle, and the distance of the deepest part of the fossa to the mental foramen on both sides based on the patients' age.

Variable	Side	Age	Mean ± standard deviation	P-value
Fossa depth	right	<36	1.59 ± 0.51	0.005
		36-50	1.85 ± 0.43	
		>50	1.89 ± 0.47	
	left	<36	1.53 ± 0.47	0.050
		36-50	1.70 ± 0.36	
		>50	1.80 ± 0.64	
Fossa angle	right	<36	39.81 ± 4.06	0.080
		36-50	41.75 ± 5.33	
		>50	42.45 ± 5.44	
	left	<36	40.20 ± 4.15	0.184
		36-50	39.91 ± 5.08	
		>50	42.16 ± 5.05	
Distance to mental foramen	right	<36	16.67 ± 1.83	0.992
		36-50	16.72 ± 2.07	
		>50	16.70 ± 1.96	
	left	<36	16.42 ± 2.05	0.801
		36-50	16.48 ± 2.32	
		>50	16.82 ± 2.46	

Table 4. The position of the deepest part of the fossa with the alveolar canal on the right ad left sides based on sex.

sex	Right side			Left side		
	Superior	Adjacent	Inferior	Superior	Adjacent	Inferior
Male	15	39	5	12	45	2
Female	25	37	4	23	39	4
Total	40	76	9	35	84	6
P-value	0.384			0.115		

Table 5. The starting point of concavity on both sides based on sex.

sex	Right side			Left side		
	superior 1/3	Middle 1/3	Inferior 1/3	Superior 1/3	Middle 1/3	Superior 1/3
Male	25	32	2	24	33	2
Female	24	40	2	29	35	2
Total	49	72	4	53	68	4
P-value	0.840			0.945		

as the depth increases, so does the angle of the fossa. In line with these findings, Ramasmawy et al. and Bayrak et al. also suggested that the average depth of the fossa was more on the right side of both sexes [13, 14]. On the other hand, Yildiz et al. found a mean fossa depth of 2.673 (ranging from 1.1 to 4.6) on the right side and 2.578 (ranging from 1.1 to 4.5) on the left side, which was higher than the current study [15].

Not enough studies have been conducted about the mandibular lingual concavity located in the anterior area. In a study, Kamburoğlu et al. assessed the sublingual and submandibular regions' predominance and discovered that the sublingual region's mean volume and depth were 26.5 mm and 1.3 mm, respectively [16].

Serious implications may arise for the patient in the event of lingual plate concavity perforation. The lingual artery emerges from the external carotid artery and curves around to cross the genioglossus and hyoglossus muscles. There may be a chance of perforation in the front portion of the jaw due to a wide lingual concavity. Ventral tongue piercing of the vasculature can result in potentially deadly arterial bleeding [10, 17].

A lingual plate concavity perforation in the posterior area is not as dangerous. With the exception of lymph nodes and submandibular glands, the submandibular area contains very few crucial structures. Nonetheless, this does not imply that implant placement in this region should be disregarded. During surgery in the posterior mandible, the lingual nerve's position needs to be taken into account. A branch of the mandibular nerve's posterior trunk, the lingual nerve, originates in the infratemporal fossa and runs near the mandible's lingual aspect around the third molar. Perforation of the lingual cortical plate after implantation can cause nerve dysfunction because of the lingual nerve's variable path.

If an implant is inserted into a lingual plate perforation without being noticed, the extruded implant could result in infection or chronic inflammation [10, 18].

According to this study, men have a deeper fossa than women. This may indicate that, compared to female individuals, the thickness and width of the bone is less in male patients at this stage. Additionally, the relationship between the mandibur canal and the depth of the submandibular gland cavity was equal to the superior relationship on the left and right sides of the mandible in women. However, compared to the right side, the left side exhibits more parallel and inferior relationships. Men's left and right sides of the mandible have equal relationships between the depth of the submandibular gland cavity and the mandibular canal in superior, inferior, and parallel relationships [13].

While some investigations have suggested that the average values of submandibular gland cavity depth in women are greater on the right side than on the left side [9, 13], others have not observed significant differences in terms of fossa depth between men and women [19, 20]. The average depth of submandibular depression in Kamburolu et al.'s study was 2.4 mm. The average depth of right and left submandibular and sublingual recesses were 2.26 mm, 2.24 mm, and 0.58 mm for women and 2.57 mm, 2.68 mm, and 0.81 mm for men, respectively [21]. Additionally, Yoon et al.'s study found that on the right side, the average depth of concavity was 3.55 mm for women and 3.93 mm for men, and on the left, it was 3.74 mm for women and 4.15 mm for men [10]. The variations among these studies could be related to ethnic variances.

Based on our findings, the average angle of the fossa on both sides in men and women did not significantly differ. The average fossa angle between men and women was not significantly different in Haghanifar et al.'s study on the left side, but a significant difference was noted between the sexes on the right side [4]. In the Panjnoush et al.'s study, female patients had a larger average concavity angle [22]. The differing measurement techniques used in the present investigation may be attributed to this discrepancy. In Chan et al.'s study, although the mean depth of the submandibular gland fossa was identical in both sexes, the mean fossa concavity angle was larger in male patients [23]. These variations may be due to different measurement approaches, imaging methodologies, and various anatomical features in different individuals.

The current study found no significant distinction in terms of the distance of the deepest part of the fossa to the mental foramen based on sex and age. In line with these findings, Vhatkar et al. obtained a average distance of 24.5 ± 5.5 mm in patients over 35 years old and 23.0 ± 6.8 mm in those below 35 years old, which was not significantly different [20]. Moreover, the mean distance between the deepest part of the fossa to the mental foramen was calculated as 17.3 ± 8.12 mm in Parnia et al.'s investigation, which was not significantly different regarding the side of the mandible and the individuals' age [19].

Although the present investigation suggested a significant difference in the average fossa depth on both sides in different age groups (under 36, 36-50, and over 50), Bayrak et al.'s investigation suggested contradicting results [14]. Their study classified patients as three different age groups of: under 20, 20-44, and over 45. This discrepancy may result from different age classifications and study-related demographic variances.

Another feature discovered by the present study was that the deepest part of the fossa on both sides was more adjacent to the canal. However, Haghanifar et al. reported it to be above the canal on both sides and sexes [4]. Furthermore, other studies have suggested that the beginning of the concavity was mainly in the middle 1/3 in both sides with no significant difference in men and women [4, 13], which was in line with our findings.

Before implant insertion, the depth of the submandibular gland cavity at the posterior region of the mandible must be detected since lack of identification can cause perforation of the lingual plate. The bottom of the mouth may bleed as a result of this injury. Since the mandibular symphysis contains branches of the sublingual, submental, and mylohyoid arteries, perforation of the molar region can be a major complication. Therefore, the diameter of the implant should be determined prior to implantation based on the height and depth of the mandibular bone in the submandibular gland cavity to reduce the possibility of a perforation [24].

According to the findings, the mean fossa depth was 1.80 mm and 1.70 mm on the right and left sides, respectively, which can increase the risk of bleeding and potentially fatal perforations of the lingual cortical plate and the branches of the sublingual artery during surgery. Therefore, prior to performing implant surgery in the posterior parts of the mandible, a thorough assessment of the morphology and size of the submandibular cavity is crucial.

5. Limitations

One of the constraints of the present study was the lack of high-quality CBCT images to evaluate the submandibular fossa accurately. Further investigations with proper equipment are required to confirm the current findings.

6. Conclusion

A thorough assessment of the jaw for proper detection of anatomical landmarks is essential prior to implantation. To evaluate the mandible for dental implantation, CBCT offers precise mandibular anatomy and submandibular gland cavity depth. In this research, it was found that the depth of the submandibular gland cavity was higher in men compared to women. Compared to the left side, the right side of the mandible has a deeper fossa. Therefore, while designing an implant in the right posterior portion of the male mandible, significant caution should be exercised.

Acknowledgment

This study has been carried out in the Dental Faculty at Mazandaran University, which deserves a great appreciation for all academic and financial support.

Authors' contribution

Alireza Khodabakhshian: Data curation
Melika Mollaei: Writing-Original draft
Mona Alimohammadi: Visualization
Fatemeh Ghobadi: Visualization
Abolfazl Hosseinnataj: Software
Atefeh Gholampour: Conceptualization, Methodology

Conflict of Interest

None.

Funding/support

None.

ORCID

Alireza Khodabakhshian https://orcid.org/0009-0001-1640-7548
Melika Mollaei https://orcid.org/0000-0002-5012-3872
Mona Alimohammadi https://orcid.org/0000-0003-1708-2375
Fatemeh Ghobadi https://orcid.org/0000-0001-6117-1864
Abolfazl Hosseinnataj https://orcid.org/0000-0003-0549-1788
Atefeh Gholampour https://orcid.org/0000-0002-3170-8517

References

1. Safi Y, Amid R, Vasegh Z. Anatomical variations in the interforaminal regions of candidates for implant-assisted overdentures: a cross-sectional CBCT analysis. General dentistry. 2020;68(6):11-6.

2. Tomasi C, Derks J. Etiology, occurrence, and consequences of implant loss. Periodontology 2000. 2022;88(1):13-35.
3. Nickenig H-J, Wichmann M, Eitner S, Zoeller JE, Kreppel M. Lingual concavities in the mandible: a morphological study using cross-sectional analysis determined by CBCT. Journal of Cranio-Maxillofacial Surgery. 2015;43(2):254-9.
4. Haghanifar S, Arbabzadegan N, Moudi E, Bijani A, Nozari F. Evaluation of lingual mandibular depression of the submandibular salivary glands using cone-beam computed tomography. Res Med Dent Sci. 2018;6:563-7.
5. Sadeghi F, Mirhadi S, Malekzadeh J, Gholami SA. Evaluation of Submandibular Gland Fossa Variety by CBCT in Patient Referring to Oral and Maxillofacial Radiology Center in Yasuj in the Academic Year of 2017-2018. International Journal of Pharmaceutical Research (09752366). 2020;12(1).
6. Borahan M, Dönmez F, Ulay G, Sadıkoğlu A, Pekiner F. Assesment of submandibular fossa depth using cone beam computed tomography. Yeditepe Dental Journal. 2018;14:51-6.
7. Chan HL, Benavides E, Yeh CY, Fu JH, Rudek IE, Wang HL. Risk assessment of lingual plate perforation in posterior mandibular region: a virtual implant placement study using cone-beam computed tomography. Journal of periodontology. 2011;82(1):129-35.
8. Saha N, Nair V. Role of CBCT in Dental Implant Treatment Plan: A Review. Journal of Medicine and Health Research. 2023:1-5.
9. de Souza LA, Assis NMSP, Ribeiro RA, Carvalho ACP, Devito KL. Assessment of mandibular posterior regional landmarks using cone-beam computed tomography in dental implant surgery. Annals of Anatomy-Anatomischer Anzeiger. 2016;205:53-9.
10. Yoon TY, Patel M, Michaud RA, Manibo AM. Cone beam computerized tomography analysis of the posterior and anterior mandibular lingual concavity for dental implant patients. Journal of Oral Implantology. 2017;43(1):12-8.
11. SG K, Sushmitha S. Assessment of submandibular fossa for dental implants–A retrospective 3 dimensional cone beam computed tomographic study. Int J Curr Adv Res. 2018;7:16632-5.
12. Farahani FM, Ghaffari R, Farhad S. Evaluation of the height, depth and angle of submandibular gland fossa and cor-relation of depth with mandibular canal position using Cone beam computed to-mography. 2023.
13. Ramaswamy P, Saikiran C, Raju BM, Swathi M, Teja DD. Evaluation of the depth of submandibular gland fossa and its correlation with mandibular canal in vertical and horizontal locations using CBCT. Journal of Indian Academy of Oral Medicine and Radiology. 2020;32(1):22.
14. Bayrak S, Demirturk-Kocasarac H, Yaprak E, Ustaoglu G, Noujeim M. Correlation between the visibility of submandibular fossa and mandibular canal cortication on panoramic radiographs and submandibular fossa depth on CBCT. Med Oral Patol Oral Cir Bucal. 2018;23(1):e105-e11.
15. Yildiz S, Bayar GR, Guvenc I, Kocabiyik N, Cömert A. Tomographic evaluation on bone morphology in posterior mandibular region for safe placement of dental implant. Surgical and Radiologic Anatomy. 2015;37(2):167-73.
16. Kamburoğlu K, Acar B, Yüksel S, Paksoy CS. CBCT quantitative evaluation of mandibular lingual concavities in dental implant patients. Surgical and Radiologic Anatomy. 2015;37:1209-15.
17. Gakonyo J, Butt F, Mwachaka P, Wagaiyu E. Arterial blood supply variation in the anterior midline mandible: Significance to dental implantology. International journal of implant dentistry. 2015;1:1-5.
18. Bokindo IK, Butt F, Hassanali J. Morphology and morphometry of the lingual nerve in relation to the mandibular third molar. Open Journal of Stomatology. 2015;5(1):6-11.
19. Parnia F, Fard EM, Mahboub F, Hafezeqoran A, Gavgani FE. Tomographic volume evaluation of submandibular fossa in patients requiring dental implants. Oral Surgery, Oral Medicine, Oral Pathology, Oral Radiology, and Endodontology. 2010;109(1):e32-e6.
20. Vhatkar BS, Shetty NK, Waghmare MS, Pagare SS, Vahanwala SP, Santosh V. Submandibular Gland Fossa Assessment with Cone Beam Computed Tomography. INTERNATIONAL JOURNAL OF SCIENTIFIC STUDY. 2019;7(4):53-7.
21. Kamburoğlu K, Acar B, Yüksel S, Paksoy CS. CBCT quantitative evaluation of mandibular lingual concavities in dental implant patients. Surgical and Radiologic Anatomy. 2015;37(10):1209-15.
22. Panjnoush M, Eil N, Kheirandish Y, Mofidi N, Shamshiri AR. Evaluation of the concavity depth and inclination in jaws using CBCT. Caspian Journal of Dental Research. 2016;5(2):17-23.
23. Chan HL, Brooks SL, Fu JH, Yeh CY, Rudek I, Wang HL. Cross-sectional analysis of the mandibular lingual concavity using cone beam computed tomography. Clinical oral implants research. 2011;22(2):201-6.
24. Alsharif SB, Bahanan L, Almutairi M, Alshammry S, Khalifa H. Retrospective Assessment Of Dental Implant-Related Anatomical Structure Perforations Using Cone Beam Computed Tomography. Annals of Dental Specialty Vol. 2023;11(1):22.

Please cite this paper as: Khodabakhshian A, Mollaei M, Alimohammadi M, Ghobadi F, Hosseinnataj A, Gholampour A. Assessing the Variations of the Depth and Angle of the Submandibular Gland Fossa and Its Correlation with the Mandibular Canal Using Cone Beam Computed Tomography (CBCT). Journal of "Regeneration, Reconstruction & Restoration"(Triple R). 2024; Volume 9: e4. Doi: 10.22037/rrr.v9.44263